On generalized reciprocal diagrams for self-stressed frameworks

Andrea Micheletti

Department of Civil Engineering - University of Rome "Tor Vergata"
Via Politecnico 1, 00133, Rome, Italy
micheletti@ing.uniroma2.it

Abstract

We present the duality between edge lengths and axial forces in self-stressed frameworks, upon which are based reciprocal diagrams, introduced by Maxwell and Cremona in the nineteenth century. The main concepts and principles are simplified by using a graph theoretic approach. We describe some unusual orthogonality relations, involving lengths, axial forces and their rates of change.

Reciprocal diagrams, which exist for frameworks with underlying planar graph, are extended also to the non-planar case by introducing a new criterion. When this criterion can be applied, different reciprocals can be obtained as symmetric frameworks. The same criterion can also be applied to planar cases giving new reciprocals as a result.

Although reciprocal diagrams cannot be obtained for all self-stressed frameworks, the presented duality always holds and it provides useful insights for design and form-finding purposes.

1 INTRODUCTION

Reciprocal diagrams for pin-connected frameworks has been established by Maxwell [1, 2] and by Cremona [3] for solving problems of statics graphically. They showed that a two-dimensional framework possesses a self-stress if and only if there is a reciprocal framework, with edge lengths equal to the axial forces in the original framework. The two frameworks are the projection on the plane of two dual, or polar, polyhedra, where each vertex of one polyhedron corresponds to a face of the other one and vice-versa. Not too long ago, Crapo and Whiteley reformulated reciprocal diagrams in a more rigorous way and studied their generalization to three-dimensional structures [4, 5, 6]. More recently, Erdahl et al. [7] studied higher-dimensional generalizations. Reciprocal diagrams have also been used in scene analysis to check whether

a given drawing is the exact projection of a polyhedral surface [8]. In a recent application, they served for the static analysis of vaulted masonry constructions [9].

We make a step further on the generalization of reciprocal diagrams in three dimensions. By using basic concepts in graph theory, we state the algebraic duality between edge lengths and axial forces in a self-stressed framework, which is valid in any dimension. Reciprocal frameworks, as discovered by Maxwell and Cremona, are obtained when the graph underlying the framework is planar, i.e. this graph can be drawn on the plane without edge intersections. We then introduce a new criterion to find reciprocal frameworks which works for some non-planar graphs. This criterion can be applied also in the planar case in order to find new reciprocals. Notice that, in our terminology, the adjective *planar* always refers to the above mentioned property of a graph, while the adjectives *two-dimensional*, *three-dimensional* refer to the Euclidean space where the framework is considered.

In this work, we do not make use of the correspondence between reciprocal diagrams and polyhedral projections. We adopt Cremona's construction, in which the edges of the reciprocal framework are parallel to the edges of the original one; this is equivalent to Maxwell's construction in which pairs of corresponding edges are orthogonal to each other. Throughout the paper, we will refer to [10, 11, 12, 13], for graph theoretic notions and methods, and to [14, 15, 16], for algebraic notions regarding pin-connected frameworks.

2 THE PLANAR CASE

To give the intuition about reciprocal diagrams and to introduce notation and basic results, we refer to a simple example. Figure 1 (left) depicts both a pin-connected framework and its representation as an oriented graph. If the four nodes lay on the same plane, the structure has one self-stress state, up to a scaling factor, which is represented in Fig. 1 (center); thicker lines in the graph correspond to compressed edges.

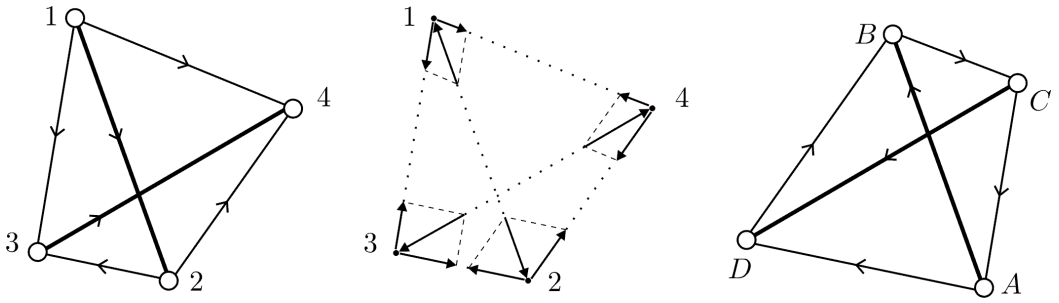

Figure 1: A framework with planar graph (left) and its self-stress state (center). The corresponding reciprocal framework (right). Corresponding edges are parallel to each other.

In our notation, we use latin subscripts for quantities related to the nodes of the framework and greek subscripts for quantities related to the edges. When necessary we denote an edge by the ordered pair of nodes it connects. We use latin superscripts to specify quantities measured along cartesian coordinate directions.

We denote by $\boldsymbol{p}_i \in \mathbb{R}^3$ the nodal position vector of node i in a cartesian reference frame and by $\boldsymbol{e}_{ij} \in \mathbb{R}^3$ the unit vector directed from $\boldsymbol{p}_i$ to $\boldsymbol{p}_j$,

$$\boldsymbol{e}_{ij} = \frac{\boldsymbol{p}_j - \boldsymbol{p}_i}{\|\boldsymbol{p}_j - \boldsymbol{p}_i\|}\,, \tag{1}$$

so that $\boldsymbol{e}_{ij} = -\boldsymbol{e}_{ji}$. The axial force, or *stress*, carried by the edge connecting nodes i and j is denoted by $t_{ij} = t_{ji}$, positive if the edge is in traction. The equilibrium equation of node i subjected only to the axial forces of the edges it connects is written as

$$\sum_j t_{ij}\,\boldsymbol{e}_{ji} = \boldsymbol{0}\,, \tag{2}$$

where the summation is extended to all nodes j connected to node i by an edge. For example, the equilibrium equation for node 2 is

$$t_{21}\frac{\boldsymbol{p}_2 - \boldsymbol{p}_1}{\|\boldsymbol{p}_2 - \boldsymbol{p}_1\|} + t_{23}\frac{\boldsymbol{p}_2 - \boldsymbol{p}_3}{\|\boldsymbol{p}_2 - \boldsymbol{p}_3\|} + t_{24}\frac{\boldsymbol{p}_2 - \boldsymbol{p}_4}{\|\boldsymbol{p}_2 - \boldsymbol{p}_4\|} = \boldsymbol{0}\,. \tag{3}$$

For the purposes of this paper, the nodal equilibrium equations of a framework are written in terms of the quantities related to the oriented graph underlying the framework. A *graph* is a collection of vertices together with a collection of edges which connects pairs of distinct vertices. Two or more edges can connect the same pair of vertices; however, this does not happen in our examples. A graph is *oriented* if an orientation is assigned to each edge, *i.e.* an ordering of the two vertices it connects. We say that an edge *leaves* the first vertex and *enters* the second vertex. For the graph underlying a framework, there is a one-to-one correspondence between vertices of the graph and the nodes of the framework, so that corresponding edges connect corresponding pairs of nodes and vertices.

For an oriented graph with n vertices and e edges, the *incidence matrix* $\boldsymbol{C}_0$ is an n by e matrix whose (i,α) entry, $c_{i\alpha}$, can be defined as

$$c_{i\alpha} = \begin{cases} 1 & \text{if edge } \alpha \text{ enters vertex } i \\ -1 & \text{if edge } \alpha \text{ leaves vertex } i \\ 0 & \text{if edge } \alpha \text{ is not incident on vertex } i \end{cases}\,; \tag{4}$$

notice that sometimes in the literature the opposite signs are used in this definition, as the two choices are equivalent. The incidence matrix for the graph in Figure 1 (left) is written as follows.

$$\boldsymbol{C}_0 = \begin{array}{c} \begin{matrix} \text{(edges)} & 12 & 13 & 14 & 23 & 24 & 34 \end{matrix} \\ \begin{bmatrix} -1 & -1 & -1 & 0 & 0 & 0 \\ 1 & 0 & 0 & -1 & -1 & 0 \\ 0 & 1 & 0 & 1 & 0 & -1 \\ 0 & 0 & 1 & 0 & 1 & 1 \end{bmatrix} \end{array} \begin{matrix} \text{(vertices)} \\ 1 \\ 2 \\ 3 \\ 4 \end{matrix} \tag{5}$$

Notice that each column of this matrix has exactly two nonzero entries which are equal to 1 and -1, consequently, the row vectors sum up to the null vector in $\mathbb{R}^e$. In other words, one row vector is linearly dependent on the others. If the graph is connected the rank of the incidence matrix is $(n-1)$ [11]. A graph is connected if there are paths formed by vertices and edges going from one vertex to all the others.

We denote $\boldsymbol{e}_\alpha \in \mathbb{R}^3$ the unit vector parallel to the direction of edge α, with same orientation, so that if this edge is oriented from vertex i to vertex j we have $\boldsymbol{e}_\alpha = \boldsymbol{e}_{ij}$. If t_α is the axial force carried by edge α then the equilibrium equation of node i, under no external force, is written as

$$\sum_\alpha c_{i\alpha} t_\alpha \boldsymbol{e}_\alpha = \boldsymbol{0}\,. \tag{6}$$

It is easy to check that this expression is equivalent to (2).

In graph theory, the row space of the incidence matrix is called the *bond space*, or *cutset space*, a subspace of $\mathbb{R}^e$. A vector which belongs to this subspace is obtained by 'cutting' the graph drawing into two pieces with a line, the non-zero entries of this vector correspond to the cut edges and have values 1 or -1, two entries have opposite values if the corresponding edges pass through the cutting line in opposite directions. In particular, each row vector of $\boldsymbol{C}_0$ corresponds to the cut edges incident to a vertex.

The orthogonal complement of the cutset space in $\mathbb{R}^e$ is called the *cycle space*. In our example, a basis of the cycle space is given by the three row vectors of the following matrix.

$$\boldsymbol{C}^* = \begin{array}{c} \begin{matrix} \text{(edges)} & 12 & 13 & 14 & 23 & 24 & 34 \end{matrix} \\ \begin{bmatrix} -1 & 1 & 0 & -1 & 0 & 0 \\ 1 & 0 & -1 & 0 & 1 & 0 \\ 0 & -1 & 1 & 0 & 0 & -1 \end{bmatrix} \end{array} \begin{matrix} \text{(cycles)} \\ A \\ B \\ C \end{matrix} \tag{7}$$

Each element of the basis represents a *cycle* in the graph, that is a sequence of vertices and edges which forms a closed path. For example, the first row vector in (7) correspond to the cycle $1 \rightarrow 3 \rightarrow 2 \rightarrow 1$, where edges (1,3) is traversed in the same direction with respect to its orientation, while edge (1,2) and (2,3) are traversed in the direction opposite to their orientation; the non-zero entries correspond to these edges, with values 1 and -1 respectively. It is easy to check that the scalar product between any two vectors representing a cutset and a cycle is zero.

The complementarity of the cutset space and the cycle space is the first ingredient for reciprocal systems. The second one is the planarity of the underlying graph. A graph is *planar* if it can be drawn on the plane without edge intersections. The graph underlying the framework in Fig. 1 (left) is planar, as shown in Fig. 2 (left). In such a drawing, a *face* is a region of the plane bounded by the edges of the graph, including

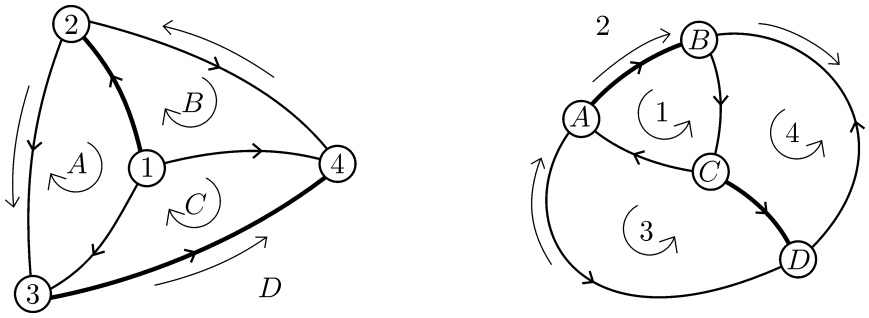

Figure 2: The dual planar graphs corresponding to the reciprocal frameworks in Fig. 1.

the exterior infinite region. Since each edge connects two vertices and it is the common boundary of two faces, we can take the faces as the vertices of a *dual* planar graph, two dual vertices are connected if the corresponding faces have an edge in common, like in Fig. 2 (right).

In a planar graph, the edges bounding a face form a cycle and we can choose the basis for the cycle space according to the following criterion.

Criterion 1. (Basis for the cycle space in the planar case.)

(a) *The basis is given by the cycles associated to all the faces except one*;

(b) *two cycles traverse a common edge in opposite directions*.

In the example, the cycles in (7) has been chosen according to this criterion, they correspond to faces A, B and C: due to (a), each edge belongs at most to two cycles in the basis, so that each column in $\boldsymbol{C}^*$ has one or two non-zero entries; due to (b), two non-zero entries in a column have opposite signs. This choice

allow us to add to the matrix in (7) another row vector for face D, which is the sum of all the row vectors changed in sign, obtaining a matrix which is the incidence matrix of the dual graph (Fig. 2 right).

$$\begin{array}{rcccccc} \text{(edges)} & 12 & 13 & 14 & 23 & 24 & 34 \\ \text{(dual edges)} & AB & CA & BC & AD & DB & CD \end{array} \quad \text{(dual vertices)}$$

$$\boldsymbol{C}_0^* = \begin{bmatrix} -1 & 1 & 0 & -1 & 0 & 0 \\ 1 & 0 & -1 & 0 & 1 & 0 \\ 0 & -1 & 1 & 0 & 0 & -1 \\ 0 & 0 & 0 & 1 & -1 & 1 \end{bmatrix} \begin{array}{c} A \\ B \\ C \\ D \end{array} \tag{8}$$

We denote by $c^*_{i\alpha}$ the (i,α) entry of the matrix $\boldsymbol{C}_0^*$ in (8). Since a cycle is a closed path formed by edges, if l_α is the length of edge α, then for each cycle we have the relation

$$\sum_\alpha c^*_{i\alpha} l_\alpha \boldsymbol{e}_\alpha = \boldsymbol{0}\,, \tag{9}$$

which has the same form of the equilibrium equation (6). This correspondence leads to the following result in the planar case, also known as the Maxwell-Cremona theorem [1, 3, 4, 5, 6].

Given a pin-connected framework with underlying planar graph, there exists a non-null self-stress state, for which (6) *is satisfied at every node, if and only if there exist a* reciprocal *framework on the dual graph with unit vectors* $\boldsymbol{e}^*_\alpha$ *satisfying*

$$\boldsymbol{e}^*_\alpha = \pm \boldsymbol{e}_\alpha \quad \forall\, \alpha\,. \tag{10}$$

The cycle space and cutset space are exchanged in the two systems. The lengths l^*_α of the reciprocal framework satisfy

$$\sum_\alpha c_{i\alpha} l^*_\alpha \boldsymbol{e}^*_\alpha = \boldsymbol{0} \quad \forall\, i\,. \tag{11}$$

In absolute value and up to a scaling factor, the stresses t^*_α and the lengths in the reciprocal framework are respectively equal to the corresponding lengths and stresses in the original framework:

$$\begin{cases} |t^*_\alpha| = l_\alpha\,, \\ l^*_\alpha = |t_\alpha|\,. \end{cases} \tag{12}$$

Corresponding edges are parallel to each other. In the reciprocal system, the unit vectors corresponding

to compressed elements in the original system have opposite orientation:

$$\begin{cases} \boldsymbol{e}_\alpha^* = \boldsymbol{e}_\alpha & \text{if } \ t_\alpha > 0\,, \\ \boldsymbol{e}_\alpha^* = -\boldsymbol{e}_\alpha & \text{if } \ t_\alpha < 0\,. \end{cases} \tag{13}$$

Two edges with stresses of opposite sign have dual stresses of opposite sign, so that

$$\sum_\alpha c_{i\alpha}^* t_\alpha^* \boldsymbol{e}_\alpha^* = \boldsymbol{0} \quad \forall\, i\,. \tag{14}$$

We remark that the lengths and the stresses satisfying (6), (9), (11), (14) can be arbitrarily scaled. Notice also that the reciprocal framework is independent from the orientation of the edges in the graph, while if we reverse the directions of all the cycles in the basis we obtain a reciprocal which is a reflection through a point of the previous one.

Figure 1 (right) shows the reciprocal framework in this example. If the nodes of the original framework do not lay on the same plane, then there is no self-stress, (10) cannot be satisfied and it is not possible to construct the reciprocal framework.

3 DUALITY BETWEEN AXIAL FORCES AND EDGE LENGTHS

Given an oriented graph, let $\boldsymbol{C}_0$ be the associated incidence matrix defined by (4). As each row vector of this matrix is dependent on the others, we denote as $\boldsymbol{C}$ the reduced matrix obtained from $\boldsymbol{C}_0$ by eliminating one row. The rows of $\boldsymbol{C}$ provide a basis for the cutset space. The basis of the cycle space is given by all the vectors which are in the null space of $\boldsymbol{C}$. By defining $\boldsymbol{C}^*$ as the matrix which contains the cycle space basis as row vectors, we can write

$$\boldsymbol{C}^* \boldsymbol{C}^T = \boldsymbol{0}\,. \tag{15}$$

By denoting with $\mathrm{Im}\,\boldsymbol{C}^T$ and $\mathrm{Ker}\,\boldsymbol{C}$ respectively the row space and the null space of the matrix $\boldsymbol{C}$, we have

$$\begin{cases} \text{cutset space}: & \mathrm{Im}\,\boldsymbol{C}^T = \mathrm{Im}\,\boldsymbol{C}_0^T = \mathrm{Ker}\,\boldsymbol{C}^* \\ \text{cycle space}: & \mathrm{Ker}\,\boldsymbol{C} = \mathrm{Ker}\,\boldsymbol{C}_0 = \mathrm{Im}\,\boldsymbol{C}^{*T} \end{cases}. \tag{16}$$

If the graph is connected, the dimensions of the cutset space and cycle space are, respectively, $(n-1)$ and $(e-n+1)$ [10, 11].

Now, let us consider a framework associated with the graph. If $\{\boldsymbol{e}^x, \boldsymbol{e}^y, \boldsymbol{e}^z\}$ are three mutually orthog-

onal unit vectors along the cartesian directions, we can define the cartesian projections of the axial force vectors and those of the length vectors as

$$s_\alpha^h := t_\alpha \boldsymbol{e}_\alpha \cdot \boldsymbol{e}^h \,, \tag{17}$$

$$d_\alpha^h := l_\alpha \boldsymbol{e}_\alpha \cdot \boldsymbol{e}^h \,, \tag{18}$$

for $h = x, y, z$. For the edge from node i to node j, the length projections can also be written as

$$d_{ij}^h = p_j^h - p_i^h \,, \tag{19}$$

where $p_i^h := \boldsymbol{p}_i \cdot \boldsymbol{e}^h$ is the cartesian coordinate of node i along direction h.

We can rewrite (6) and (9) as

$$\boldsymbol{C}\, \boldsymbol{s}^h = \boldsymbol{0} \,, \tag{20}$$

$$\boldsymbol{C}^* \boldsymbol{d}^h = \boldsymbol{0} \tag{21}$$

for $h = x, y, z$, where the vectors $\boldsymbol{s}^h$, $\boldsymbol{d}^h \in \mathbb{R}^e$ contain respectively the projections (17) and (18) along the direction h.

A physical interpretation of the cutset and cycle spaces is provided by the electrical network associated with the graph [10, 11, 12, 13]: a vector in the cutset space represents potential differences between vertices while a vector in the cycle space represents a set of currents in the edges. In the theory of electrical networks, (20) and (21) are known as Kirchhoff's laws [17], stating that the sum of the currents entering a node is equal to the sum of the currents leaving that node, and that the potential differences between the nodes of a cycle sum up to zero. In a framework, the cartesian projections of the length vectors and those of the axial force vectors correspond respectively to potential differences and to currents in the electrical network with the same underlying graph: relation (21) states the orthogonality of the former with respect to the cycle space, while (20) states the orthogonality of the latter with respect to the cutset space.

In the previous example, by considering node 1 (Fig. 3, left), from (5) and (20) along direction x, we have

$$-s_{12}^x - s_{13}^x - s_{14}^x = 0 \,,$$

while considering node 3 (Fig. 3, center) we have

$$s_{13}^x + s_{23}^x - s_{34}^x = 0 \,.$$

On the other side, considering the cycle B (Fig. 3, right), from (7) and (21) along direction x, we have

$$d^x_{12} - d^x_{14} + d^x_{24} = (p^x_2 - p^x_1) - (p^x_4 - p^x_1) + (p^x_4 - p^x_2) = 0\,.$$

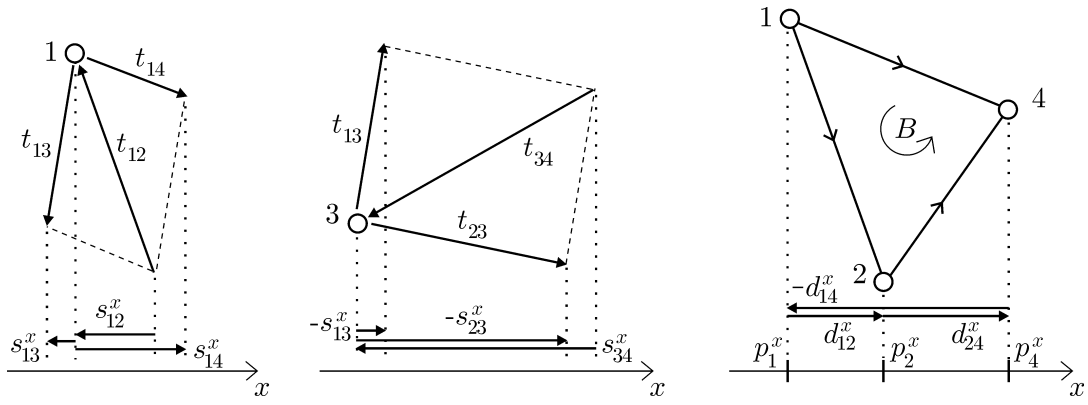

Figure 3: The cartesian projections of the axial force vectors and those of the length vectors corresponds respectively to currents and to potential differences in a corresponding electrical network.

By introducing the cartesian projections of the unit vectors of the edges,

$$n^h_\alpha = \boldsymbol{e}_\alpha \cdot \boldsymbol{e}^h\,, \tag{22}$$

and by denoting with $\boldsymbol{n}^h \in \mathbb{R}^e$ the vector containing all the projections along direction h, we can define the quantities

$$\boldsymbol{C}^h := \boldsymbol{C}(\mathrm{diag}(\boldsymbol{n}^h))\ , \quad \boldsymbol{C}^{*h} := \boldsymbol{C}^*(\mathrm{diag}(\boldsymbol{n}^h))\,, \tag{23}$$

where $\mathrm{diag}(\boldsymbol{n}^h)$ is the diagonal matrix whose entries correspond to those of $\boldsymbol{n}^h$. In this way (20) and (21) are rewritten as

$$\boldsymbol{C}^h\boldsymbol{t} = \boldsymbol{0}\ , \quad \boldsymbol{C}^{*h}\boldsymbol{l} = \boldsymbol{0}\,, \tag{24}$$

with $\boldsymbol{t}, \boldsymbol{l} \in \mathbb{R}^e$ the vectors containing the axial forces and edge lengths respectively. By collecting the previous equations along the three cartesian directions we have, respectively for $\boldsymbol{t}$ and $\boldsymbol{l}$,

$$\boldsymbol{A}\boldsymbol{t} = \boldsymbol{0}\ , \quad \boldsymbol{A}^*\boldsymbol{l} = \boldsymbol{0}\,, \tag{25}$$

where $\boldsymbol{A}$ and $\boldsymbol{A}^*$ have the form:

$$\boldsymbol{A} = \begin{bmatrix} \boldsymbol{C}^x \\ \boldsymbol{C}^y \\ \boldsymbol{C}^z \end{bmatrix} , \quad \boldsymbol{A}^* = \begin{bmatrix} \boldsymbol{C}^{*x} \\ \boldsymbol{C}^{*y} \\ \boldsymbol{C}^{*z} \end{bmatrix} . \tag{26}$$

We see that, together with the usual equilibrium matrix $\boldsymbol{A}$, whose null space contains the self-stress vectors $\boldsymbol{t}$, there exists a dual matrix $\boldsymbol{A}^*$ whose null space contains the lengths vectors $\boldsymbol{l}$. This means that, in order to have a connected structures with given edge directions $\boldsymbol{e}_\alpha$, the null space of $\boldsymbol{A}^*$ have to be non-empty.

We recall here the kinematic compatibility relations described by the transpose of the equilibrium matrix $\boldsymbol{A}^T$ [15]. The vector $\boldsymbol{p}^h \in \mathbb{R}^n$ collects the nodal coordinates p_i^h along direction h, while the vector $\boldsymbol{p} \in \mathbb{R}^{3n}$ contains all the nodal coordinates in the form

$$\boldsymbol{p} = \begin{bmatrix} \boldsymbol{p}^x \\ \boldsymbol{p}^y \\ \boldsymbol{p}^z \end{bmatrix} .$$

If $\dot{\boldsymbol{p}}$ represents the nodal velocities in a motion of the framework, then the kinematic compatibility equations are written as

$$\boldsymbol{A}^T \dot{\boldsymbol{p}} = \dot{\boldsymbol{l}} , \tag{27}$$

where $\dot{\boldsymbol{l}}$ contains the stretching velocities of the edges. For example, the equation for edge (i, j) is

$$(\dot{\boldsymbol{p}}_j - \dot{\boldsymbol{p}}_i) \cdot \boldsymbol{e}_{ij} = \dot{l}_{ij} . \tag{28}$$

3.1 Orthogonality principles

Since the cutset space and the cycle space are orthogonal complement in $\mathbb{R}^e$, (20) and (21) imply that the vectors $\boldsymbol{s}^h$ and $\boldsymbol{d}^k$ are orthogonal to each other for every $h, k = x, y, z$:

$$\boldsymbol{s}^h \cdot \boldsymbol{d}^k = 0 \quad \forall \boldsymbol{s}^h \in \mathrm{Ker}\, \boldsymbol{C} \, , \, \forall \boldsymbol{d}^k \in \mathrm{Im}\, \boldsymbol{C}^T . \tag{29}$$

This represents the well known *orthogonality principle* in electrical network theory, also known as *Tellegen's theorem* [18]. From this principle, we can derive interesting relations. By considering a second

different framework but with the same underlying graph, the following relation holds

$$\sum_h \boldsymbol{s}^h \cdot \tilde{\boldsymbol{d}}^h = \sum_\alpha t_\alpha \boldsymbol{e}_\alpha \cdot \tilde{l}_\alpha \tilde{\boldsymbol{e}}_\alpha = 0\,, \tag{30}$$

where we distinguished with a tilde the quantities of the second framework. In particular, (30) written for the self-stress and the length vectors of the same framework gives

$$\boldsymbol{t} \cdot \boldsymbol{l} = 0 \quad \forall \boldsymbol{t} \in \mathrm{Ker}\boldsymbol{A}\,,\ \forall \boldsymbol{l} \in \mathrm{Ker}\boldsymbol{A}^*\,. \tag{31}$$

This is an interesting relation for designers: it shows that when a self-stressed system have a large number of edges in traction and few edges in compression, the compressed edges are longer or/and more stressed, making their design against buckling more problematic.

An alternative way to obtain (31) is the following. Since the null space and the row space of $\boldsymbol{A}$ are mutually orthogonal we have

$$\boldsymbol{t} \cdot \dot{\boldsymbol{l}} = 0 \quad \forall \boldsymbol{t} \in \mathrm{Ker}\boldsymbol{A}\,,\ \forall \dot{\boldsymbol{l}} \in \mathrm{Im}\boldsymbol{A}^T\,; \tag{32}$$

if we take $\dot{\boldsymbol{l}} = a\boldsymbol{l}$, with $a \neq 0$ constant, which corresponds to a uniform expansion ($a > 0$) or shrinkage ($a < 0$) of the structure, we obtain (31).

It can be shown [12, 13] that the orthogonality principle is equivalent to the principle of virtual power. Indeed, (32) is equivalent to the principle of virtual power in the case of null external forces, stating that the power spent by the internal forces is null.

We notice also that relation (31) represents a discrete particular version of the Signorini's theorem in linear elasticity [19]: for a continuum body occupying the volume V under null external volume and contact forces we have

$$\int_V \boldsymbol{T} dV = \boldsymbol{0}\,, \tag{33}$$

where $\boldsymbol{T}$ is the Cauchy stress tensor. Here, for a cylindrical rod subjected only to a constant axial stress T we have

$$\int_{V_\alpha} T dV_\alpha = t_\alpha l_\alpha\,, \tag{34}$$

where $t_\alpha = TA_\alpha$ is the resultant axial force, A_α the area of the cross section of the rod and $V_\alpha = l_\alpha A_\alpha$ its volume.

Another important relation is obtained by taking the first time derivative of (31) and considering (32),

we obtain:

$$\dot{\boldsymbol{t}} \cdot \boldsymbol{l} = 0 \quad \forall\, \boldsymbol{l} \in \mathrm{Ker}\boldsymbol{A}^* \,,\ \forall \boldsymbol{t} \in \mathrm{Ker}\boldsymbol{A}\,. \tag{35}$$

This is a condition which the rate of change of the self-stress has to satisfy during a motion of the framework.

Lastly, (31), (32) and (35) together imply that the following dual relations holds:

$$\boldsymbol{l} \in \mathrm{Ker}\boldsymbol{A}^* \subset \mathrm{Im}\boldsymbol{A}^T \ni \dot{\boldsymbol{l}}\,; \tag{36}$$

$$\boldsymbol{t} \in \mathrm{Ker}\boldsymbol{A} \subset \mathrm{Im}\boldsymbol{A}^{*T} \ni \dot{\boldsymbol{t}}\,. \tag{37}$$

About the last relation, we see from (35) that $\dot{\boldsymbol{t}}$ belongs to $\mathrm{Im}\boldsymbol{A}^{*T}$. Moreover, we can choose a particular $\dot{\boldsymbol{t}} = a\boldsymbol{t}$, with $a \neq 0$ a constant, which corresponds to a uniform scaling of the self-stress; hence, the null space of $\boldsymbol{A}$ is included in the image of $\boldsymbol{A}^{*T}$.

3.2 Force-coefficient formulation

For later use in Section 4 and to make the connection with existing literature on self-stressed frameworks, we report the equations regarding the force-coefficient formulation [20, 21]. The force coefficient of edge α is defined as

$$q_\alpha := \frac{t_\alpha}{l_\alpha}\,, \tag{38}$$

so that the equilibrium equation (2) for node i is rewritten as

$$\sum_j t_{ij}\,\boldsymbol{e}_{ji} = \sum_j t_{ij}\frac{\boldsymbol{p}_i - \boldsymbol{p}_j}{l_{ij}} = \sum_j q_{ij}(\boldsymbol{p}_i - \boldsymbol{p}_j) = \boldsymbol{0}\,, \tag{39}$$

where the summation is extended to all nodes j connected to node i. The corresponding equations in terms of the incidence matrix of the structure $\boldsymbol{C}_0$ are obtained as follows. The relation between $\boldsymbol{d}^h$ and $\boldsymbol{p}^h$ is given by

$$\boldsymbol{d}^h = \boldsymbol{C}_0^T\boldsymbol{p}^h\,. \tag{40}$$

From (38) and (17), we have

$$s_\alpha^h = q_\alpha d_\alpha^h \tag{41}$$

or, by introducing the vector $\boldsymbol{q} \in \mathbb{R}^e$, containing the force coefficient of all the edges,

$$\boldsymbol{s}^h = \mathrm{diag}(\boldsymbol{q})\boldsymbol{d}^h\,. \tag{42}$$

In this way, the equilibrium equation (20) is rewritten as

$$0 = \boldsymbol{C}_0 \boldsymbol{s}^h = \boldsymbol{C}_0 \mathrm{diag}(\boldsymbol{q}) \boldsymbol{C}_0^T \boldsymbol{p}^h \,. \tag{43}$$

By denoting with $\boldsymbol{c}_\alpha$ the column vector of $\boldsymbol{C}_0$ corresponding to edge α,

$$\boldsymbol{C}_0 \equiv \begin{bmatrix} & | & \\ \cdots & \boldsymbol{c}_\alpha & \cdots \\ & | & \end{bmatrix} , \tag{44}$$

we can rewrite (43) as

$$\sum_\alpha q_\alpha \boldsymbol{c}_\alpha \boldsymbol{c}_\alpha^T \boldsymbol{p}^h = 0 \,. \tag{45}$$

where $\boldsymbol{c}_{ij} \boldsymbol{c}_{ij}^T$ is a e by e matrix whose non-null entries are only in positions ii, ij, ji, jj,

$$\boldsymbol{c}_{ij} \boldsymbol{c}_{ij}^T \equiv \begin{bmatrix} & \vdots & & \vdots & \\ \cdots & 1 & \cdots & -1 & \cdots \\ & \vdots & & \vdots & \\ \cdots & -1 & \cdots & 1 & \cdots \\ & \vdots & & \vdots & \end{bmatrix} . \tag{46}$$

The linear operators (46) associated with the columns of $\boldsymbol{C}_0$ serve also to write the kinematic compatibility equations. It is easy to see that (28) can be rewritten as

$$\sum_h \boldsymbol{c}_{ij} \boldsymbol{c}_{ij}^T \boldsymbol{p}^h \cdot \dot{\boldsymbol{p}}^h = (\dot{\boldsymbol{p}}_j - \dot{\boldsymbol{p}}_i) \cdot (\boldsymbol{p}_j - \boldsymbol{p}_i) = l_{ij} \, \dot{l}_{ij} \,. \tag{47}$$

3.3 Existence of the reciprocal

If the underlying graph of a framework is planar, then the existence of the reciprocal is equivalent to the existence of a self-stress state. We can choose the matrices $\boldsymbol{C}^*$ and $\boldsymbol{C}_0^*$, i.e. the basis for the cycle space and the dual incidence matrix, by considering the faces of a planar representation of the graph according to Criterion 1. The existence of a self-stress guarantees that there exists a dual structure with $\boldsymbol{e}_\alpha^* = \mathrm{sign}(t_\alpha) \boldsymbol{e}_\alpha$. All the previous equations are valid for the dual system by replacing $\boldsymbol{C}$ with $\boldsymbol{C}^*$ and $\boldsymbol{e}_\alpha$ with $\boldsymbol{e}_\alpha^*$. In particular, $(24)_1$ and $(24)_2$ represents the condition which the dual lengths and the dual stresses, respectively,

satisfy.

To construct the reciprocal system, we can associate one node of the dual framework to each row vector in $\boldsymbol{C}_0^*$, with nodal coordinates such as to satisfy

$$d_{ij}^{*h} = s_{ij}^h = p_j^{*h} - p_i^{*h}\,, \tag{48}$$

or,

$$\boldsymbol{d}^{*h} = \boldsymbol{s}^h = \boldsymbol{C}_0^{*T}\boldsymbol{p}^{*h}\,. \tag{49}$$

An interesting two-dimensional example is shown in Fig. 4 (left). This planar framework possesses a self-stress state only for particular nodal positions, under the geometric condition that the three axis collinear with edges α, β and γ meet at a common point, as in the figure. The reciprocal framework (Fig. 4, right) possesses two independent states of self-stresses. This means that for the original framework there are two independent length vectors satisfying $(24)_2$ and that there are multiple configurations with the same self-stress (Figure 4, center). These configurations are also known as *parallel drawings* [6].

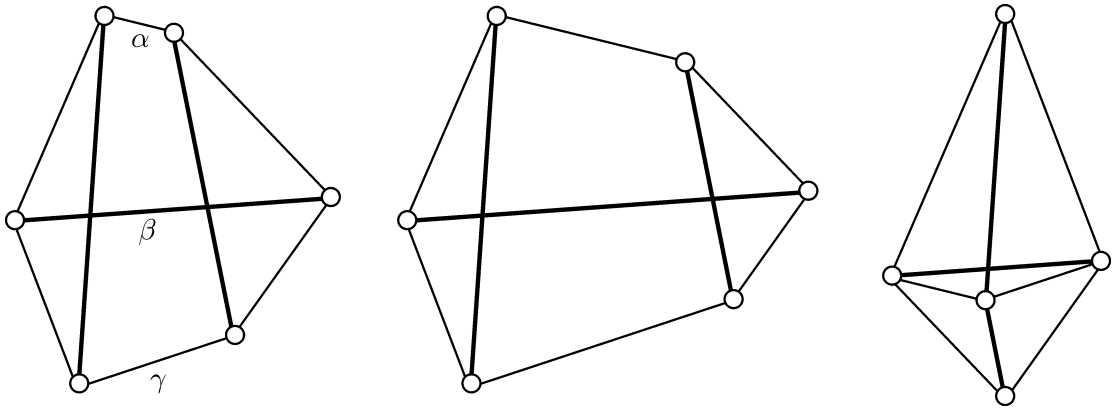

Figure 4: Two frameworks (left and center) with the same single self-stress state and the corresponding reciprocal (right) possessing two independent self-stress states.

As recalled by Crapo [4], Cremona's construction for reciprocal diagrams can be applied to three-dimensional frameworks, as long as their underlying graph is planar. For example, Fig. 5 shows the reciprocal of a classic tensegrity system.

Summarizing, the problem of finding a reciprocal of a given self-stressed framework can be solved by testing the underlying graph for planarity and, in case of a positive answer, by identifying corresponding faces in the planar graph to obtain the basis for the cycle space. Although the examples presented here have

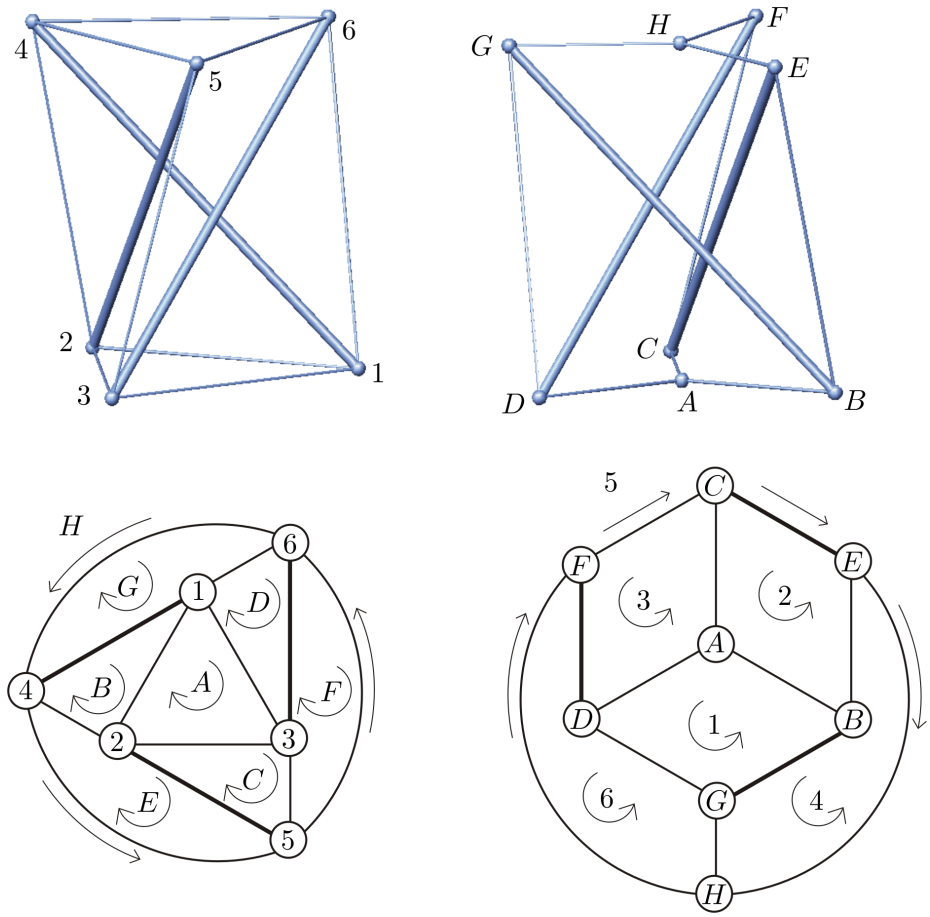

Figure 5: A tensegrity structure (top left), its reciprocal (top right) and the two corresponding planar graphs (bottom).

been worked out manually, many algorithms have been devised in graph theory and computer science to perform these operations automatically (see [22] for a review and [23] for a recent procedure).

3.4 Extended Maxwell's rule and derived relations

We here use the *Extended Maxwell's rule* [15] to derive some relations for the dimension of the fundamental subspaces associated to $\boldsymbol{A}$ and $\boldsymbol{A}^*$, for the reciprocals in the planar case. We recall that the number of independent cycles is known from the number of vertices and edges of the system,

$$c = e - n + 1\,. \tag{50}$$

We denote by s the number of independent self-stress states, $s = \dim(\mathrm{Ker}\boldsymbol{A})$, and by m the number of independent internal mechanisms, i.e. the non-rigid nodal velocities which cause no change in length of the edges. For a two-dimensional system, the extended Maxwell's rule states that

$$2n - 3 - e = m - s\,. \tag{51}$$

The same rule written for the reciprocal framework is

$$2n^* - 3 - e^* = m^* - s^*\,, \tag{52}$$

where we denoted with a star the quantities related to the reciprocal. The number of edges and nodes of the reciprocal are, respectively

$$e^* = e\ ,\ \ n^* = c + 1 = e - n + 2\,. \tag{53}$$

By using (51), (52) and (53) we easily obtain

$$m^* - s^* + m - s = -2\,. \tag{54}$$

For a three-dimensional system, the extended Maxwell's rule is written as

$$3n - 6 - e = m - s\,; \tag{55}$$

and the analogous relation holds for the reciprocal. The same computation leads, in this case, to the relation

$$m^* - s^* + m - s = e - 6\,. \tag{56}$$

We see that there is an important difference between the two cases, since in three dimensions the dimensions of the fundamental subspaces associated to $\boldsymbol{A}$ and $\boldsymbol{A}^*$ are related to the number of edges in the framework.

4 THE NON-PLANAR CASE

Many graphs are non-planar, important examples are the complete graph on five vertices, usually called K_5 (Fig. 8, left), and the complete bipartite graph on two set of three vertices, usually called K_{33} (Fig. 6, left). A graph is *complete* if every vertex is connected to all the others. A graph is *bipartite* if the vertices

are partitioned into two sets and every edge connects a vertex in one set and a vertex in the other one. A *complete bipartite* graph is a bipartite graph where every vertex in a set is connected to all the vertices in the other set. A simple characterization of planar graphs has been given by Kuratowski [10] in terms of these two graphs and can be stated as follows: *A graph is planar if and only if it does not contain a subdivision of K_{33} or K_5 as a subgraph*. A *subdivision* of a graph results from inserting vertices into edges.

For two-dimensional frameworks, Bow [24] extended reciprocal diagrams to the non-planar case by inserting an additional node at the intersection of two edges. This cannot be done in three dimensions since two crossing edges in the graph does not necessarily intersect in the framework. Another generalization to the non-planar case is described by Crapo and Whiteley [5], producing reciprocals as infinite frameworks.

Here we present a method which can be applied to some non-planar graphs to obtain reciprocals as symmetric frameworks. We illustrate the method in the case of K_{33} and K_5.

4.1 First non-planar example: K_{33}

Let us consider the system in Fig. 6 (left) with non-planar graph K_{33}. The system possesses a self-stress only for particular nodal positions. In the configuration shown, where the nodes are at the vertices of a regular hexagon, every edge carries the same axial force in magnitude; as before, thicker lines represents compressed edges.

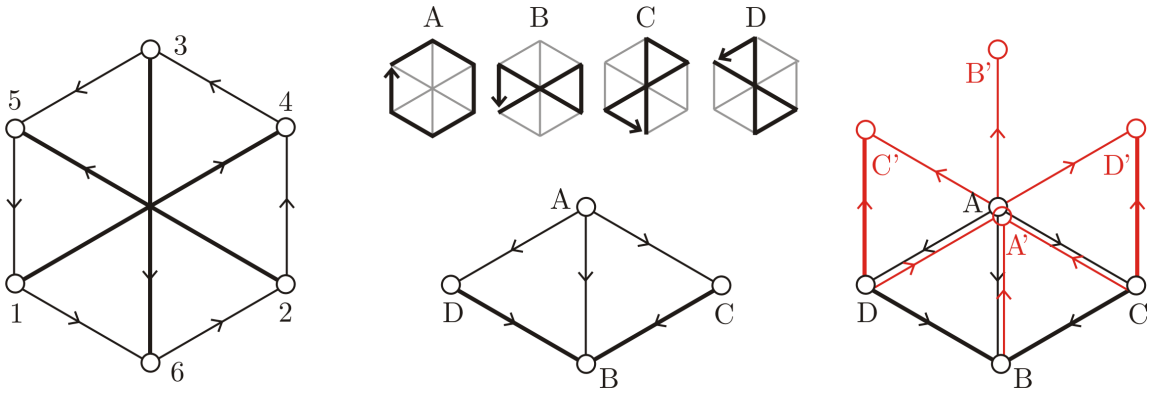

edges	14	51	16	25	62	24	36	43	35
dual edges	CB	AB	AC	DB	AD'	AB'	CD'	AC'	AD
					DA'	BA'	DC'	CA'	

Figure 6: A two-dimensional system with non-planar graph K_{33} (left). The cycle basis satisfying Criterion 2 (top center). The partial (bottom center) and full representation (right) of the dual edges corresponding to the incidence matrix (58).

The incidence matrix for the directed graph is written as follows:

$$\begin{array}{c} (\text{edges}) \\ \boldsymbol{C}_0 = \end{array} \begin{array}{c} \begin{array}{ccccccccc} 14 & 15 & 16 & 25 & 26 & 24 & 36 & 34 & 35 \end{array} \\ \left[\begin{array}{ccccccccc} -1 & 1 & -1 & 0 & 0 & 0 & 0 & 0 & 0 \\ 0 & 0 & 0 & -1 & 1 & -1 & 0 & 0 & 0 \\ 0 & 0 & 0 & 0 & 0 & 0 & -1 & 1 & -1 \\ 1 & 0 & 0 & 0 & 0 & 1 & 0 & -1 & 0 \\ 0 & -1 & 0 & 1 & 0 & 0 & 0 & 0 & 1 \\ 0 & 0 & 1 & 0 & -1 & 0 & 1 & 0 & 0 \end{array}\right] \end{array} \begin{array}{c} (\text{vertices}) \\ 1 \\ 2 \\ 3 \\ 4 \\ 5 \\ 6 \end{array} \tag{57}$$

Since the graph is not planar, it is not possible to find a basis for the cycle space satisfying Criterion 1. However, it is still possible to find a basis which satisfies the following criterion.

Criterion 2. (Basis for the cycle space in the non-planar case.)

(a) *Each edge belongs exactly to two cycles in the basis*;

(b) *two cycles share at most two edges*;

(c) *when two edges are shared by two cycles, one edge is traversed by the cycles in opposite directions, the other one is traversed by the cycles in the same direction*.

One possible choice of such a basis is given by the row vectors of the following matrix.

$$\begin{array}{c} (\text{edges}) \\ \boldsymbol{C}^* = \end{array} \begin{array}{c} \begin{array}{ccccccccc} 14 & 15 & 16 & 25 & 26 & 24 & 36 & 34 & 35 \end{array} \\ \left[\begin{array}{ccccccccc} 0 & -1 & -1 & 0 & -1 & -1 & 0 & -1 & -1 \\ 1 & 1 & 0 & 1 & 0 & -1 & 0 & 0 & 0 \\ -1 & 0 & 1 & 0 & 0 & 0 & -1 & -1 & 0 \\ 0 & 0 & 0 & -1 & -1 & 0 & -1 & 0 & 1 \end{array}\right] \end{array} \begin{array}{c} (\text{cycles}) \\ A \\ B \\ C \\ D \end{array} \tag{58}$$

In this basis we have the three cycles constituted by two opposite side of the hexagon and two diagonals plus the hexagon itself (Fig. 6, top center).

If we try to use the matrix in (58) as the incidence matrix of the reciprocal system we have the problem that some edges leave two vertices, instead of leaving one vertex and entering another. Figure 6 (bottom center) represent the substructure obtained by using the 1^{st}, 2^{nd}, 3^{rd}, 4^{th} and last column of (58) to obtain

the corresponding dual edges, as for these edges there is no such problem. Figure 6 (right) shows the edges corresponding to the remaining columns, they are drawn twice since each of them leaves two vertices; the nodes connected by these edges are denoted with an apex because they obviously do not coincide with the previous ones. Now, we can observe that the pairs of homologue nodes with and without apices are placed symmetrically with respect to a common point. In fact it can be shown that (58) represents the incidence matrix of a symmetric framework, where a reflection through a point leaves the framework unchanged and symmetric edges have same length and stress. Figure 7 gives a better idea of such a symmetric system in an irregular case.

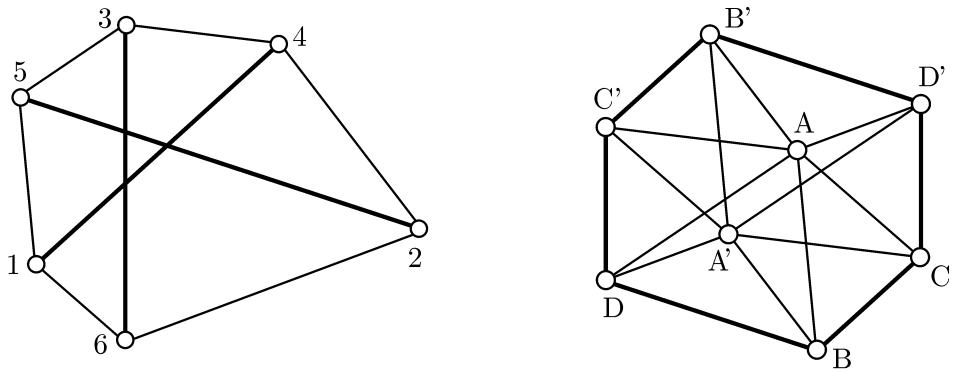

edges	14	51	16	25	62	24	36	43	35
dual edges	CB	AB	AC	DB	AD'	AB'	CD'	AC'	AD
	B'C'	B'A'	C'A'	B'D'	DA'	BA'	DC'	CA'	D'A'

Figure 7: A representation of the dual structure for the system in Fig. 6 in an irregular case.

To check this, let us consider the equilibrium equations of the dual structure in Fig. 7. To simplify the computations we take the origin of coordinates in the center of symmetry of the system. According to (39), the equilibrium equations of node C is written as follows:

$$q^*_{CA}(\boldsymbol{p}^*_C - \boldsymbol{p}^*_A) + q^*_{CB}(\boldsymbol{p}^*_C - \boldsymbol{p}^*_B) + q^*_{CA'}(\boldsymbol{p}^*_C - \boldsymbol{p}^*_{A'}) + q^*_{CD'}(\boldsymbol{p}^*_C - \boldsymbol{p}^*_{D'}) = \mathbf{0}\,. \tag{59}$$

Since the system is symmetric, we have $\boldsymbol{p}^*_{A'} = -\boldsymbol{p}^*_A$, $\boldsymbol{p}^*_{D'} = -\boldsymbol{p}^*_D$ and the previous equation becomes

$$q^*_{CA}(\boldsymbol{p}^*_C - \boldsymbol{p}^*_A) + q^*_{CB}(\boldsymbol{p}^*_C - \boldsymbol{p}^*_B) + q^*_{CA'}(\boldsymbol{p}^*_C + \boldsymbol{p}^*_A) + q^*_{CD'}(\boldsymbol{p}^*_C + \boldsymbol{p}^*_D) = \mathbf{0}\,. \tag{60}$$

The same equation is arrived at by considering the equilibrium of node C' and the symmetry conditions

$$q^*_{ij} = q^*_{i'j'} \ , \quad \boldsymbol{p}^*_i = -\boldsymbol{p}^*_{i'} \, . \tag{61}$$

The third and fourth term of (60) show that (58) represents indeed the incidence matrix of a symmetric system, as the columns of this matrix with entries of the same sign provide operators $\boldsymbol{c}^*_\alpha \boldsymbol{c}^{*\,T}_\alpha$ of the form

$$\boldsymbol{c}^*_\alpha \boldsymbol{c}^{*\,T}_\alpha \equiv \begin{bmatrix} & \vdots & & \vdots & \\ \cdots & 1 & \cdots & 1 & \cdots \\ & \vdots & & \vdots & \\ \cdots & 1 & \cdots & 1 & \cdots \\ & \vdots & & \vdots & \end{bmatrix} . \tag{62}$$

This fact is confirmed by looking at the kinematic compatibility equations. Considering edge CA', or edge $C'A$, equation (47) is written as

$$l_{CA'}\, \dot{l}_{CA'} = (\dot{\boldsymbol{p}}_C - \dot{\boldsymbol{p}}_{A'}) \cdot (\boldsymbol{p}_C - \boldsymbol{p}_{A'}) = (\dot{\boldsymbol{p}}_C + \dot{\boldsymbol{p}}_A) \cdot (\boldsymbol{p}_C + \boldsymbol{p}_A) = \sum_h \boldsymbol{c}^*_{34} \boldsymbol{c}^{*\,T}_{34} \boldsymbol{p}^h \cdot \dot{\boldsymbol{p}}^h \, . \tag{63}$$

All the static and kinematic relations of the symmetric framework can be expressed through the incidence matrix (58). Moreover, it can be seen the rows of the matrix $\boldsymbol{C}_0$ corresponds to pairs of symmetric cycles.

4.2 Second non-planar example: K_5

We pass now to consider the two-dimensional system in Fig. 8 (left) whose non-planar graph is the complete graph on five vertices K_5. The nodes of the structure are placed at the vertices of a regular pentagon. There are three independent self-stress states. For simplicity, we choose a self-stress in which the sides of the pentagon have the same positive stress and the other edges have the same negative stress. The equilibrium of node 3 is depicted in Fig. 8 (center).

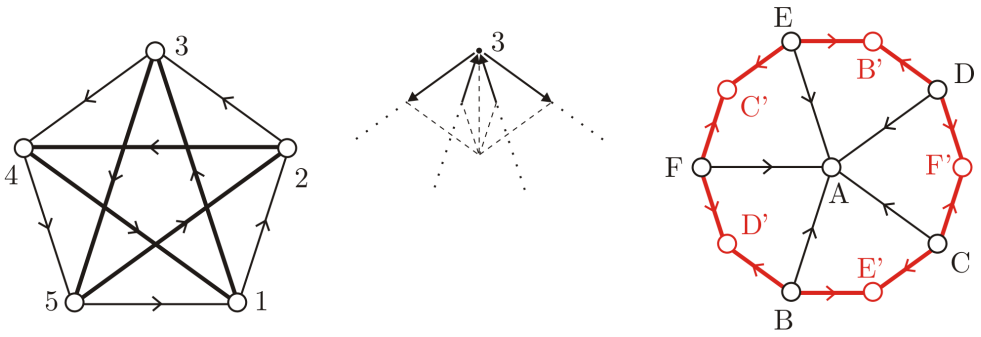

edges	12	13	23	24	34	35	45	41	51	52
dual edges	BA	DF' FD'	CA	BE' EB'	DA	CF' FC'	EA	BD' DB'	FA	CE' EC'

Figure 8: A two-dimensional system with non-planar graph K_5 (left). The equilibrium of node 3 in a symmetric self-stress state (center). The representation of the dual edges corresponding to the incidence matrix (65) (right).

The incidence matrix of the oriented graph is

$$\begin{array}{c} \text{(edges)} \\ \boldsymbol{C}_0 = \end{array} \begin{array}{c} \begin{array}{cccccccccc} 12 & 13 & 23 & 24 & 34 & 35 & 45 & 41 & 51 & 52 \end{array} \\ \left[\begin{array}{cccccccccc} -1 & -1 & 0 & 0 & 0 & 0 & 0 & 1 & 1 & 0 \\ 1 & 0 & -1 & -1 & 0 & 0 & 0 & 0 & 0 & 1 \\ 0 & 1 & 1 & 0 & -1 & -1 & 0 & 0 & 0 & 0 \\ 0 & 0 & 0 & 1 & 1 & 0 & -1 & -1 & 0 & 0 \\ 0 & 0 & 0 & 0 & 0 & 1 & 1 & 0 & -1 & -1 \end{array}\right] \end{array} \begin{array}{c} \text{(vertices)} \\ 1 \\ 2 \\ 3 \\ 4 \\ 5 \end{array} \tag{64}$$

Like before, we can choose a basis for the cycle space satisfying Criterion 2.

$$\begin{array}{c} \text{(edges)} \\ \boldsymbol{C}^* = \end{array} \begin{array}{c} \begin{array}{cccccccccc} 12 & 13 & 23 & 24 & 34 & 35 & 45 & 41 & 51 & 52 \end{array} \\ \left[\begin{array}{cccccccccc} 1 & 0 & 1 & 0 & 1 & 0 & 1 & 0 & 1 & 0 \\ -1 & 0 & 0 & -1 & 0 & 0 & 0 & -1 & 0 & 0 \\ 0 & 0 & -1 & 0 & 0 & -1 & 0 & 0 & 0 & -1 \\ 0 & -1 & 0 & 0 & -1 & 0 & 0 & -1 & 0 & 0 \\ 0 & 0 & 0 & -1 & 0 & 0 & -1 & 0 & 0 & -1 \\ 0 & -1 & 0 & 0 & 0 & -1 & 0 & 0 & -1 & 0 \end{array}\right] \end{array} \begin{array}{c} \text{(cycles)} \\ A \\ B \\ C \\ D \\ E \\ F \end{array} \tag{65}$$

Here we have the five cycles constituted by one side of the pentagon and two diagonals plus the pentagon itself. Figure 8 (right) depicts a representation of the dual edges obtained from this matrix like in the previous example. Figure 9 shows a corresponding symmetric structure in an irregular case; notice that we depicted one of the three independent parallel drawings of the reciprocal.

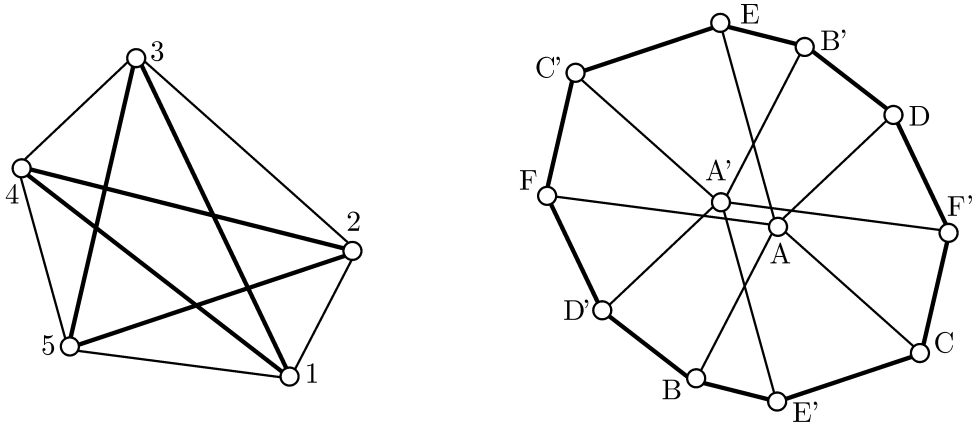

edges	12	13	23	24	34	35	45	41	51	52
dual edges	BA	DF'	CA	BE'	DA	CF'	EA	BD'	FA	CE'
	A'B'	FD'	A'C'	EB'	A'D'	FC'	A'E'	DB'	A'F'	EC'

Figure 9: A representation of the dual structures for the system in Fig. 8 in an irregular case.

Figure 10 (left) shows a three-dimensional self-stressed framework, with the shape of double pyramid, which has K_5 as underlying graph and one independent self-stress state. Figure 10 (right) shows the reciprocal system obtained by using the same choice (65) for the basis of the cycle space.

4.3 Existence of the symmetric reciprocal

In the planar case, the choice of the basis satisfying Criterion 1 leads always to a unique reciprocal system, not considering the reverse choice of the cycle directions. In the non-planar case, a basis of the cycle space satisfying Criterion 2, if it is possible, is not necessarily unique; consequently we can have many different reciprocals for a given self-stressed framework. Criterion 2 can also be applied to a planar system. For example, for the tensegrity framework in Fig. 5 we can obtain the reciprocals in Fig. 11 by choosing the bases displayed. Different possibilities exist also for the other examples in this paper.

Notice that it is not always possible to find a basis satisfying Criterion 2. A simple example is given by K_7, the complete graph on seven vertices. There are $e = 21$ edges in this graph; from Criterion 2(a) the sum of the edges in the cycles in the basis is $2e = 42$. Since the dimension of the cycle space is

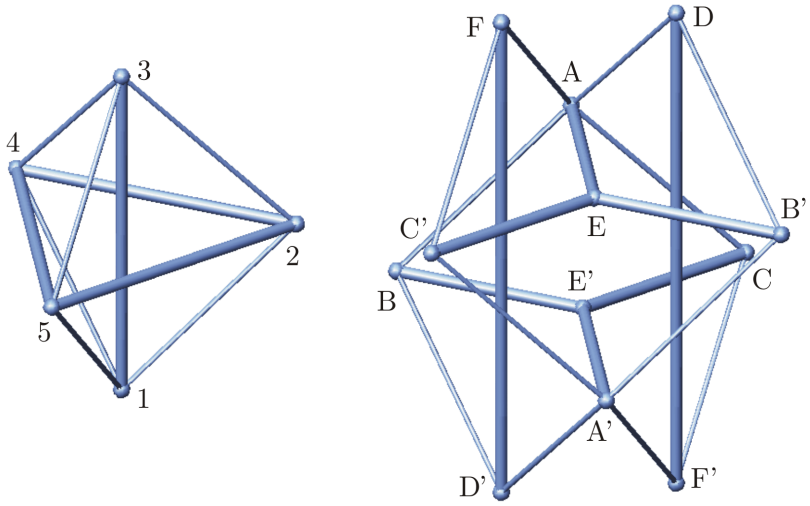

edges	12	13	23	24	34	35	45	41	51	52
dual edges	BA	DF'	CA	BE'	DA	CF'	EA	BD'	FA	CE'
	A'B'	FD'	A'C'	EB'	A'D'	FC'	A'E'	DB'	A'F'	EC'

Figure 10: A three-dimensional self-stressed system with non-planar graph K_5 and a possible dual system as a symmetric structure.

$c = 21 - 7 + 1 = 15$ and each cycle contains at least three edges, we have that the sum of the edges in a basis is greater than or equal to 45 and hence there is no basis satisfying Criterion 2.

The problem of the existence of a basis satisfying Criterion 2 has not been studied yet. This problem is related to an important conjecture in graph theory, the so-called *cycle double cover conjecture* [25], which is stated as: "*For a graph with no bridges, it is always possible to find a set of cycles where each edge is traversed by exactly two of them*". A *bridge* is an edge whose removal disconnects the graph. This conjecture has not been proven yet. However, Criterion 2 provides us a different problem as it requires that the set of cycles is also a basis of the cycle space and, moreover, that two cycles share no more than one edge traversed with same directions and no more than one edge traversed with opposite directions.

5 CONCLUSIONS

We presented the principles and the basic concepts of reciprocal diagrams for self-stressed frameworks by means of simple graph theoretic tools. After introducing the case of an underlying planar graph, we rigorously described the algebraic duality between edge lengths and axial forces, which always holds for

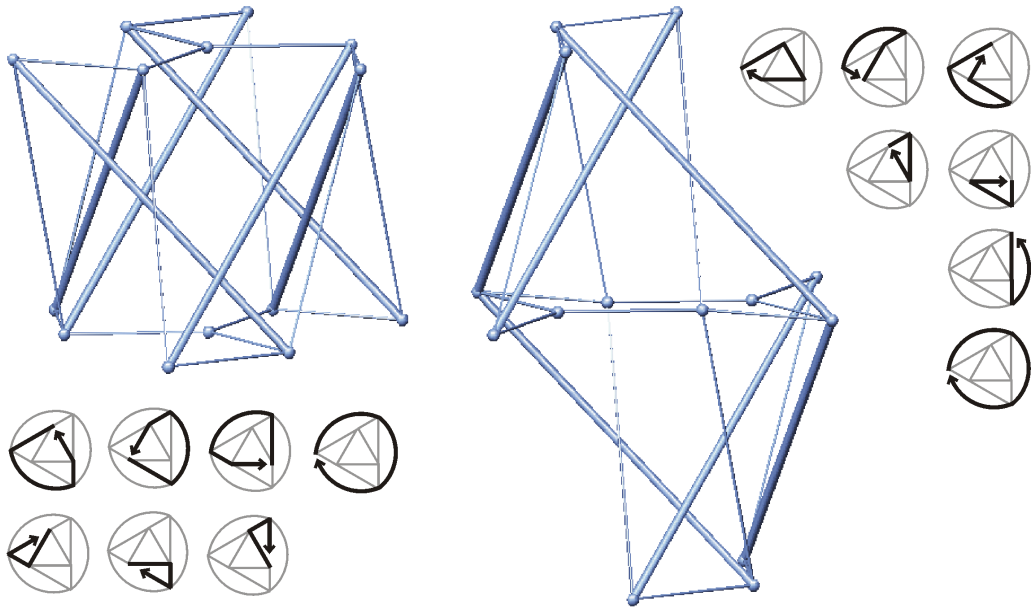

Figure 11: Two symmetric reciprocals for the tensegrity module in Fig. 5 (left), obtained with cycle bases chosen according to Criterion 2.

self-stressed systems. In particular, we stated a new orthogonality condition, dual of the virtual power principle, involving the rate of change of the self-stress during a motion. We extended reciprocal diagrams to the non-planar case by establishing a criterion for the choice of the cycle basis, which can be used to discover new reciprocals both in the planar and in the non-planar case. This criterion cannot be applied to every non-planar graph. Nevertheless, the duality can still be exploited for the design and form-finding of these systems, without the need of a graphical representation of the reciprocal and without choosing a particular basis for the cycle space.

Regarding future improvements, further studies can be done to find the conditions for which this criterion can be applied to a certain graph and to find an algorithm to select a basis. About external forces, in two dimensions they can be easily included by introducing an additional vertex, the equilibrium equations of the corresponding fictitious node represent the external balance of forces, but the details of such a procedure in three dimensions still have to be outlined. Another important issue is the stability of the reciprocal.

ACKNOWLEDGEMENTS

The author would like to thank Professor Henry Crapo for the important suggestions received. Earlier useful discussions with Professors Maurizio Angelillo, Giampietro Del Piero and Giuseppe Tomassetti are gratefully acknowledged.

References

[1] Maxwell, J. C., On reciprocal figures and diagrams of forces, Philosophical Magazine, 1864, 4, 250–261.

[2] Maxwell, J. C., On reciprocal diagrams, frames and diagrams of forces, Transactions of the Royal Society of Edinburgh, 1869, 26, 1–40.

[3] Cremona, L., Graphical Statics, English translation, Oxford University Press London (1890), 1872.

[4] Crapo, H., Structural rigidity, Structural Topology, 1979, 1, 26–45.

[5] Crapo, H. and Whiteley, W., Plane self stresses and projected polyhedra i: the basic pattern, Structural Topology, 1993, 20, 55–78.

[6] Crapo, H. and Whiteley, W. Spaces of stresses, projections and parallel drawings for spherical polyhedra, Contributions to Algebra and Geometry, 1994, 35, 259–281.

[7] Rybnikov, K. A., Erdahl, R. M. and Ryshkov, S. S., On traces of d-stresses in the skeletons of lower dimensions of homology d-manifolds. European Journal of Combinatorics, 2001, 22(6), 801–820.

[8] Huffman, D. A., A duality concept for the analysis of polyhedral scenes, in: Elcock, E. W. and Michie, D., eds., Machine Intelligence, Vol. 8,. Wiley, New York, 1977.

[9] Block, P. and Ochsendorf, J., Thrust network analysis: a new methodology for three-dimensional equilibrium, Journal of the International Association for Shell and Spatial Structures, 2007, 48, 167–173.

[10] Bondy, J. A. and Murty, U. S. R., Graph Theory with Applications, Elsevier, New York, 1976.

[11] Biggs, N., Algebraic Graph Theory, Cambridge University Press, Cambridge, UK, 1993.

[12] McPhee, J. J., On the use of linear graph theory in multibody system dynamics, Nonlinear Dynamics, 1996, 9, 73–90.

[13] Shai, O., Deriving structural theorems and methods using Tellegen's theorem and combinatorial representations, International Journal of Solids and Structures, 2001, 38, 8037–8052.

[14] Calladine, C. R., Buckminster Fuller's 'tensegrity' structures and Clerk Maxwell's rules for the construction of stiff frames, International Journal of Solids and Structures, 1978, 14, 161–172.

[15] Pellegrino, S. and Calladine, C. R., Matrix analysis of statically and kinematically indeterminate frameworks. International Journal of Solids and Structures, 1986, 22, 409–428.

[16] Calladine, C. R. and Pellegrino, S., First-order infinitesimal mechanisms, International Journal of Solids and Structures, 1991, 27, 505–515.

[17] Kirchhoff, G., Ueber den Durchgang eines elektrischen Stromes durch eine Ebene, insbesondere durch eine kreisförmige, Annalen der Physik und Chemie, 1845, 140/64(4), 497-514.

[18] Tellegen, B. D. H., A general network theorem with applications, Philips Research Report, 1952, 7, 259–269. Annals of Discrete Mathematics, 1985, 27, 1–12.

[19] Signorini, A., Sollecitazioni Iperastatiche, Rendiconti del Reale Istituto Lombardo, 1932, 2(65), 1–7.

[20] Linkwitz, K. and Schek, H. J. Einige bemerkungen zur berechnung von vorgespanten seilnetzkonstruktionen. Ingenieur–Archiv, 40:145–158, 1971.

[21] Schek, H. J., The force density method for formfinding and computation of general networks, Computer Methods in Applied Mechanics and Engineering, 1974, 3, 115–134.

[22] Tamassia, R., Di Battista, G., Eades, P. and Tollis I. G., Algorithms for drawing graphs: an annotated bibliography, Computational Geometry: Theory and Applications, 1994, 4, 235–282.

[23] Boyer, J. M. and Myrvold, W. J., On the cutting edge: Simplified o(n) planarity by edge addition, Journal of Graph Algorithms and Applications, 2004, 8(3), 241–273.

[24] Bow, R., Economics of Construction in Relation to Framed Structures. E and F.N. Spon, London, 1873.

[25] Jaeger, F., A survey of the cycle double cover conjecture, Annals of Discrete Mathematics, 1985, 27, 1–12.